Scientific Research Publishing

World Journal of Engineering and Technology, 2023, 11, 1000-1011
https://www.scirp.org/journal/wjet
ISSN Online: 2331-4249
ISSN Print: 2331-4222

Numerical Investigation of Flow Separation Control over an NACA0018 Airfoil Using Sweeping Jet Actuator

Chuanyu Gao, Tong Zhao, Lei Ding, Yalei Bai

College of Aerospace Engineering, Nanjing University of Aeronautics and Astronautics, Nanjing, China
Email: 2296468902@qq.com

How to cite this paper: Gao, C.Y., Zhao, T., Ding, L. and Bai, Y.L. (2023) Numerical Investigation of Flow Separation Control over an NACA0018 Airfoil Using Sweeping Jet Actuator. *World Journal of Engineering and Technology*, **11**, 1000-1011.
https://doi.org/10.4236/wjet.2023.114066

Received: October 9, 2023
Accepted: November 27, 2023
Published: November 30, 2023

Abstract

As an active flow control technology and with the advantages of no moving components, the Sweeping jet actuator has become a hotspot in the field of flow control. However, the linear relationship between oscillation frequency and momentum coefficient in a sweeping jet actuator makes it difficult to determine the dominant factors that affect control effectiveness. Decoupling the oscillation frequency and momentum coefficient, as well as determining the control mechanism, is the focus of studying the sweeping jet actuator. In this study, a novel sweeping jet actuator is designed using synthetic jets instead of feedback channels and applied to the flow separation control of NACA0018 airfoil. This article studies the control effect under three oscillation frequencies of $F^+ = f \times c/U_\infty = 1$, 10, 100 and three momentum coefficients of C_μ = 0.45%, 0.625%, 0.9%. The numerical results indicate that all three oscillation frequencies have good control effects on flow separation, and the control effect is best when $F^+ = 1$, with the maximum lift coefficient increasing by approximately 14% compared to the other two cases. And the sweeping jet actuator has a better ability to control flow separation as the momentum coefficient increases. By decoupling the characteristics of the sweeping jet actuator and conducting numerical analysis of the flow control effect, it will promote its better engineering application in the field of flow control.

Keywords

Flow Control, Sweeping Jet Actuator, Oscillation Frequency, Momentum Coefficient

1. Introduction

The characteristic of high lift systems in aircraft aerodynamics technology is to

increase lift while reducing drag, thereby optimizing aerodynamic efficiency and reducing fuel consumption. However, at high angles of attack and deflection, high lift systems are prone to separation in the boundary layer. Therefore, how to delay or regulate the separation of airflow is a key issue in aircraft aerodynamics research.

Flow control technology is mainly divided into two categories: active control and passive control [1]. Passive flow control, such as vortex generators [2], ribs [3], slats [4], etc., is widely used in the field of fluid dynamics due to its simple design and no need for additional energy. However, passive control lacks the ability to autonomously adjust according to changes in conditions, and in some cases, the control effect may not meet the target requirements.

Active control includes blowing and suction [5], plasma control [6], synthetic jet [7], etc. Sweeping jet actuator is a typical active control technology that converts a stable jet into an oscillating jet by utilizing flow instability. This feature of avoiding moving components during the driving process not only ensures improved energy efficiency, but also extends the service life of the equipment. These benefits make sweeping jet actuator a focus of research in the field of flow control.

Florian Ostermann [8] conducted experimental research on the complex interaction between low-frequency oscillating jets and external flow. Research has shown that the velocity of oscillating jets rapidly decays while exhibiting a high entrainment rate. It is worth noting that at lower Strouhal numbers, the spatial oscillating jet exhibits a similar effect to the jet generated by vortex over time, thus forming a vortex like flow structure over time. On the contrary, at higher Strouhal numbers, the transverse flow cannot synchronize with the motion of the jet, resulting in a stable wake in the downstream region of the jet flow field.

Daniel J Portillo [9] conducted experimental research on sweeping jet actuator and systematically analyzed their oscillation frequencies, oscillation angles, and modal structures at different scales. The research results clearly indicated that the oscillation frequency is directly proportional to the flow velocity and inversely proportional to the size of the characteristic scale. In addition, the article emphasized that the oscillation angle is inversely proportional to the flow velocity, but positively correlated with the size of the scale. These results were consistent with the relevant conclusions drawn by Bartosz J Slupski [10] and Seo [11] regarding the oscillation frequency.

Arpit Chaudhary [12] studied the experimental verification of the effect of oscillating jets on the separation control of the leading edge boundary layer of NACA0015 wings. Research has found that oscillating jets effectively delay the stall angle of attack by 6˚. And this study found that optimizing the spacing between actuator heavily depends on factors such as driving momentum and jet span coverage.

Sun Qixiang *et al.* [13] optimized the internal flow loss and stagnation time of a sweeping jet actuator by studying its geometric shape, and explored the rela-

tionship between inflow velocity, geometric shape, and oscillation frequency. Zou Jiupeng *et al.* [14] studied that the main reasons for the energy loss of the sweeping jet actuator were insufficient total pressure and poor continuity, and improved the efficiency by introducing high total pressure gas. Zhou Luanliang *et al.* [15] studied the frequency-pressure characteristics of a sweeping jet actuator under high-frequency and high-speed fluid conditions.

In the study of oscillatory jets, the main models include traditional double feedback actuator, single feedback actuator, and non-feedback actuator. The shapes of these three models are shown in **Figure 1**. However, it is not feasible to decouple the oscillation frequency and momentum coefficient in these models.

This article designs a new type of non-feedback channel sweeping jet actuator to explore the impact of the individual characteristic of the sweeping jet actuator on the flow control effect. Compared with traditional actuators, this model decouples frequency and momentum coefficients by replacing feedback channels with synthetic jets. And the article uses numerical simulation technology to apply this model to the flow control of NACA0018 airfoil, in order to evaluate the impact of oscillation frequency and momentum coefficient on the flow control effect.

2. Model Design and Method of numerical simulation

The sweeping jet actuator model used in this article is shown in **Figure 2** The model thickness is set to 1 mm, where the synthetic jets A and B are designed as the sum of stable and fluctuating flows. The simplified waveforms of synthetic jet A and B are shown in Equation (1) and Equation (2) respectively:

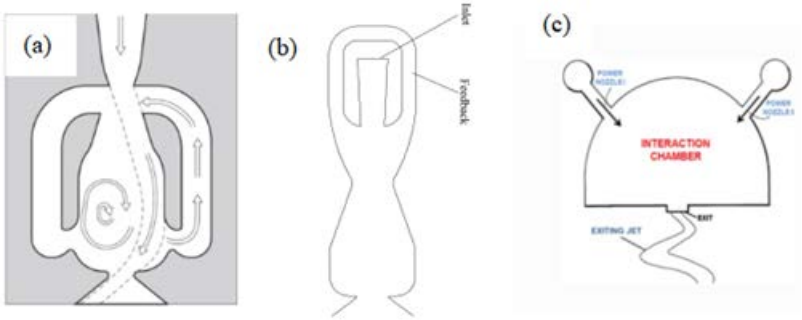

Figure 1. Traditional sweeping jet actuator models.

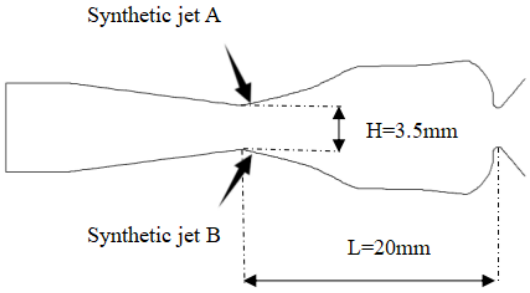

Figure 2. Model diagram of sweeping jet actuator.

$$f(x) = \mathrm{a}\sin(2\pi f^{+}t) + b \tag{1}$$

$$f(x) = -\mathrm{a}\sin(2\pi f^{+}t) + b \tag{2}$$

Figure 3 shows the internal velocity changes and corresponding Fourier transform of the sweeping jet actuator at $F^{+} = 1$. It is worth noting that the frequency of the flow field is closely consistent with the specified frequency, which proves the ability of this method to successfully decouple frequency and momentum coefficient. This observation emphasizes the effectiveness of the design.

Figure 4 shows the computational domain and grid of the sweeping jet actuator. The outer region of the computational domain is rectangular in layout and uses a quadrilateral structured grid. The number of encrypted grids during calculation is approximately 400,000.

This example uses the Large Eddy Simulation (LES) turbulence model and a pressure based time dependent solver. The working fluid is air. The constant time step is $t = 10^{-5}$ seconds, and the pressure is discretized using second-order discretization. Density, momentum, and turbulent kinetic energy are discretized using a second-order upwind formula. For boundary conditions, the main inlet and the inlet of synthetic jets A and B are set as velocity inlet and perpendicular to the boundary, the outlet is set as pressure outlet, and the remaining boundaries are set as non slip wall surfaces.

Figure 5 shows the calculation results of fluid motion in a sweeping jet actuator

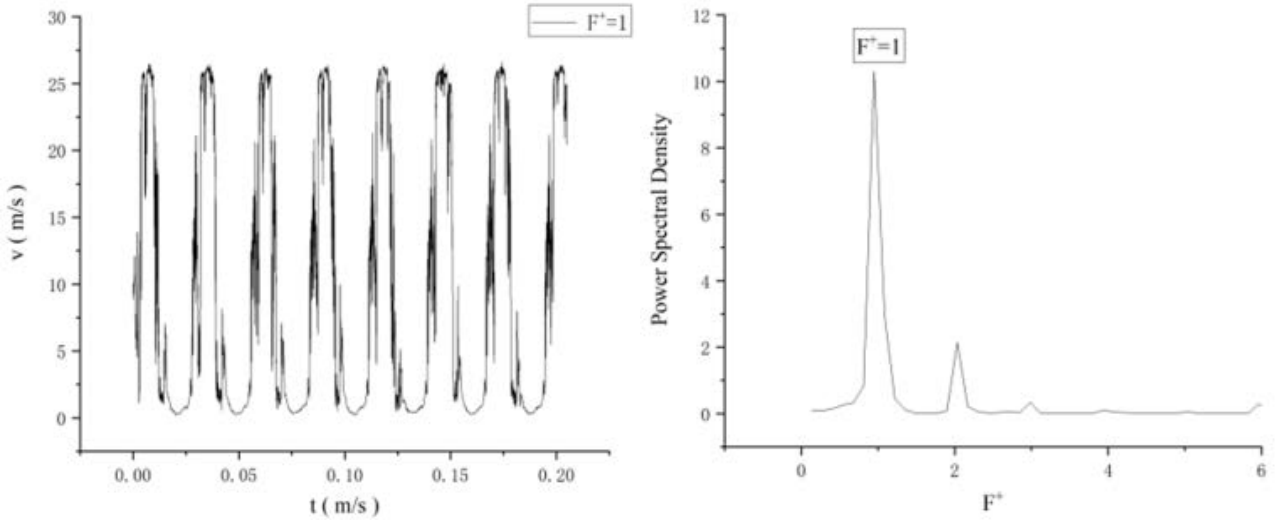

Figure 3. Internal velocity and corresponding Fourier transform of sweeping jet actuator.

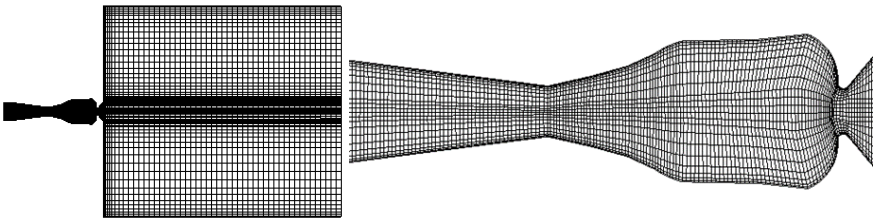

Figure 4. Computing domain and computing grid.

within one cycle. When T* = 0, the jet adheres to the lower wall, and due to the interaction between the jet and the wall, the direction of the jet at the outlet position is upward. Subsequently, the synthetic jet B began to function and generate a separated vortex. The separation vortex, which is increased by the energy of synthetic jet B, pushes the jet towards the upper wall. When T* = 1/2T, it can be observed that the jet is completely attached to the upper wall and its direction at the outlet position becomes downward. When the synthetic jet A begins to function, the jet begins to move towards the lower wall again. When T* = T, the device achieves cyclic oscillation and completes the entire cycle.

This article selects the NACA0018 airfoil as the reference airfoil, with a chord length of 250 mm and a wingspan of 100 mm. The sweeping jet actuator is installed at a 45˚ angle to the inflow direction at 0.08 x/c on the leading edge of the wing. As shown in **Figure 6**, there are a total of 6 actuators with a spacing of 15

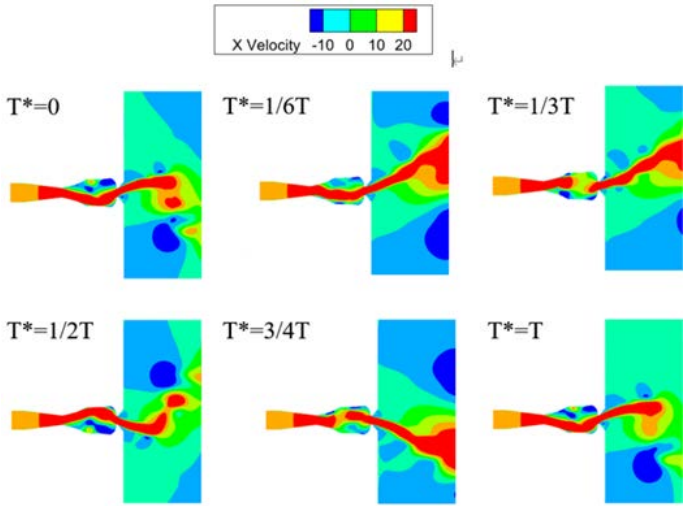

Figure 5. Flow chart of a sweeping jet actuator within one cycle.

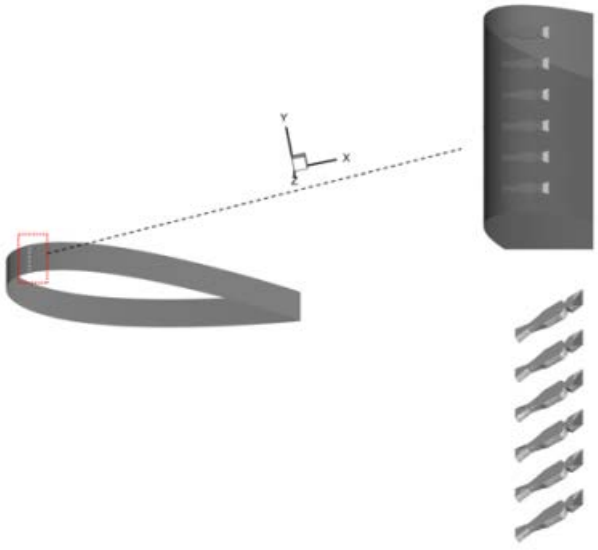

Figure 6. The Distribution of actuators on NACA0018.

mm between them. **Figure 7** shows the computational grid of the airfoil.

Comparing the calculated lift coefficient of the airfoil with the experimental results [16] in **Figure 8**, it can be seen that the trend of lift coefficient variation is consistent, and the lift coefficient reaches its maximum value at an angle of attack of 15˚. This result verifies the feasibility of the methods and grids used in numerical simulations.

Figure 9 depicts the average flow velocity and shear stress flow field of the NACA0018 airfoil at an attack angle of 18˚. It can be observed that the shear layer moves away from the airfoil surface from the middle part, resulting in a separation zone and a decrease in lift coefficient.

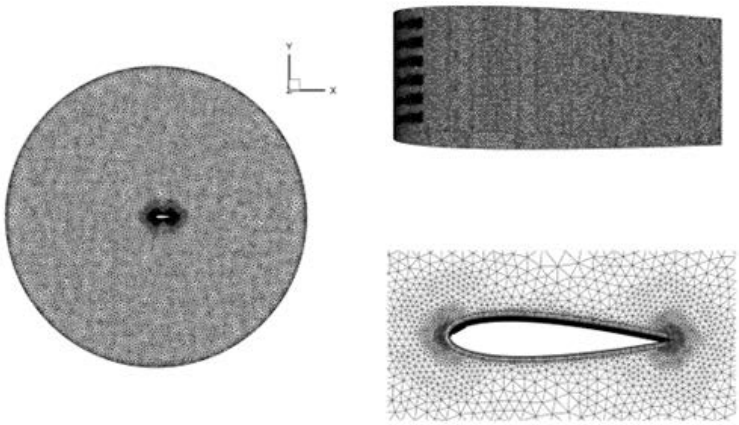

Figure 7. Calculation grid of airfoil.

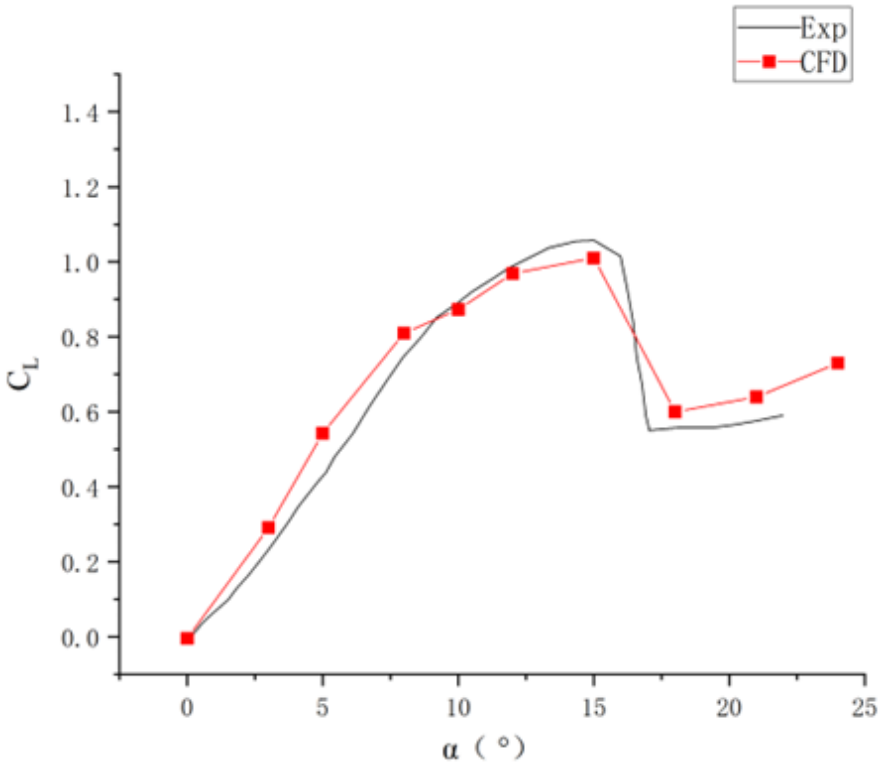

Figure 8. Lift coefficient varies with angle of attack.

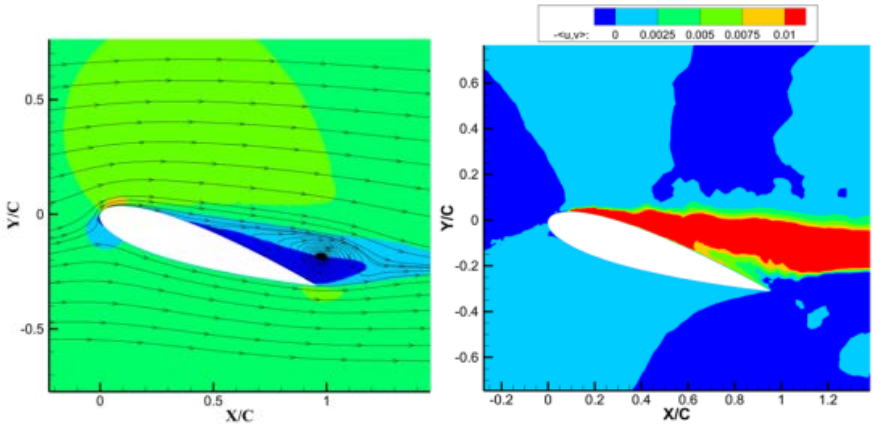

Figure 9. Average flow velocity and shear stress flow field at an angle of attack of 18˚.

3. Analysis of Flow Control Effect

For the flow situation of NACA0018, this article analyzes the flow control effect at three oscillation frequencies $F^+ = f \times c/U_\infty = 1$, 10, 100, and three momentum coefficients $C_\mu = 0.45\%$, 0.625%, 0.9%. The formula for momentum coefficient is as follows:

$$C_\mu = \frac{m * U_{jet}}{q * A_{ref}} = \frac{(\rho_{jet} * U_{jet} * n * A_{nozzle}) * U_{jet}}{(0.5 * \rho_\infty * U_\infty{}^2)(c * n * \Delta z)} = 2 * \frac{\rho_{jet} * A_{nozzle} * U_{jet}{}^2}{\rho_\infty * U_\infty{}^2 * c * \Delta z} \tag{3}$$

$$U_{jet} = \frac{m}{\rho_{jet} * A_{jet}} = \frac{m}{\rho_\infty * A_{jet}} \tag{4}$$

$$C_\mu = 2 * \frac{A_{nozzle}}{c * \Delta z} (\frac{U_{jet}}{U_\infty})^2 \tag{5}$$

Among them, A_{ref} is the reference area, which is the product of chord length and effective span, A_{nozzle} is the throat area of the oscillating jet nozzle, n is the number of actuators, Δz is the jet spacing, c is the chord length of the airfoil, and the jet nozzle is set $\rho_{jet} = \rho_\infty$.

Figure 10 shows the variation of lift coefficient of NACA0018 with angle of attack under different momentum coefficients and oscillation frequencies. When the momentum coefficient is 0.45%, several frequencies can delay the stall angle of attack by 3˚. Under this momentum coefficient, the increase in lift coefficient at $F^+ = 1$ is not significant compared to other frequencies. However, when the momentum coefficients are 0.625% and 0.9%, the increase in lift coefficient at $F^+ = 1$ is very significant. The maximum lift coefficient has increased by approximately 14% compared to the other two frequencies.

3.1. The Influence of Momentum Coefficient on Control Effectiveness

In order to study the influence of momentum coefficients on flow control, this section analyzes the flow control effects of several momentum coefficients at the same frequency when the oscillation frequency $F^+ = 1$.

Figure 11 shows the average velocity field at an 18˚ angle of attack under

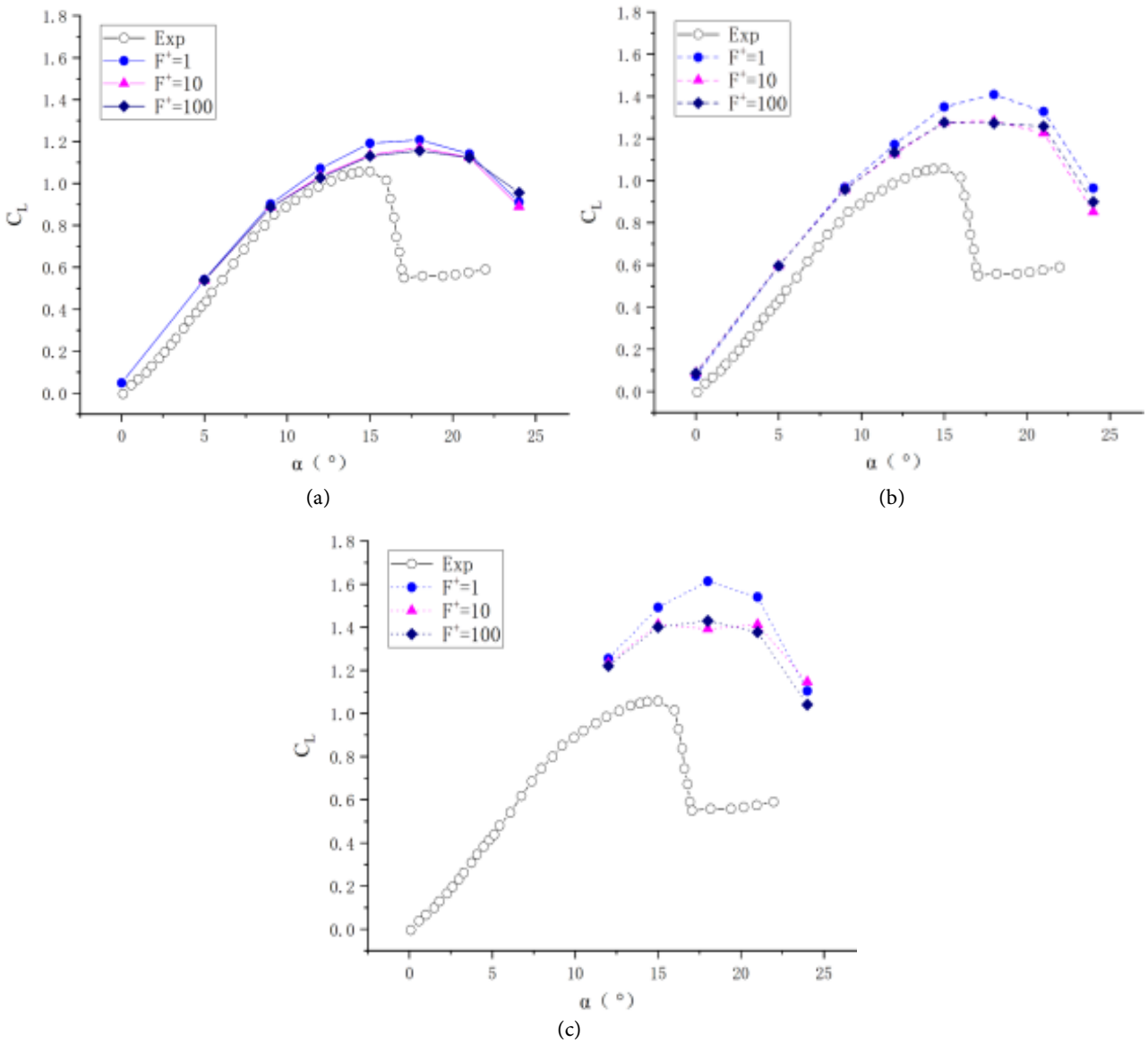

Figure 10. The variation of lift with angle of attack under different momentum coefficients and oscillation frequencies. (a) Control effect of each frequency when $C_\mu = 0.45\%$; (b) Control effect of each frequency when $C_\mu = 0.625\%$; (c) Control effect of each frequency when $C_\mu = 0.9\%$.

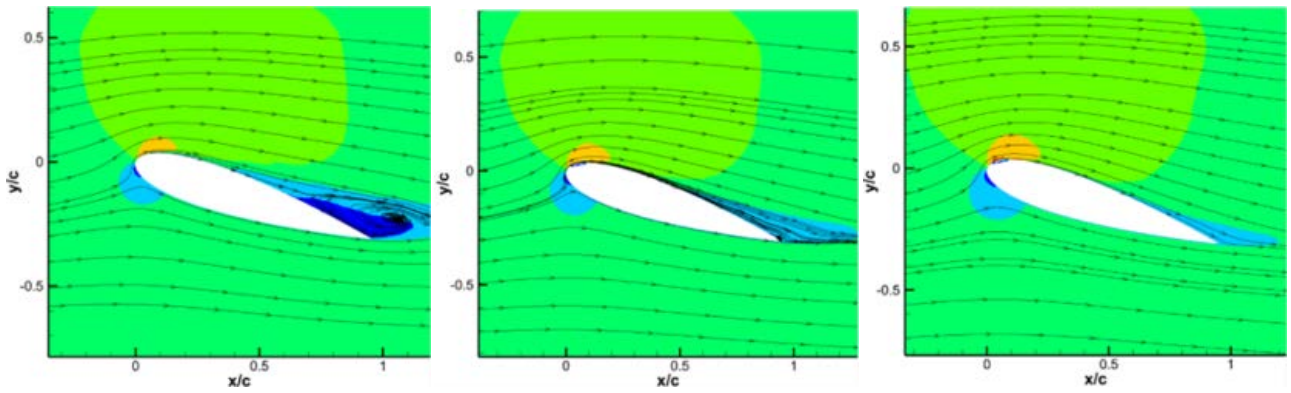

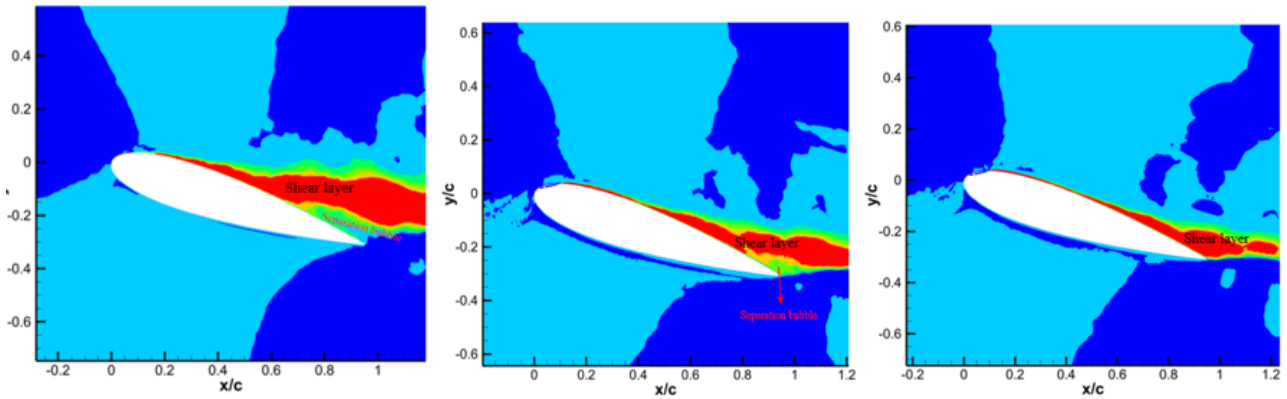

Figure 11. Average velocity and flow field at momentum coefficients of 0.45% (left), 0.625% (middle), and 0.9% (right).

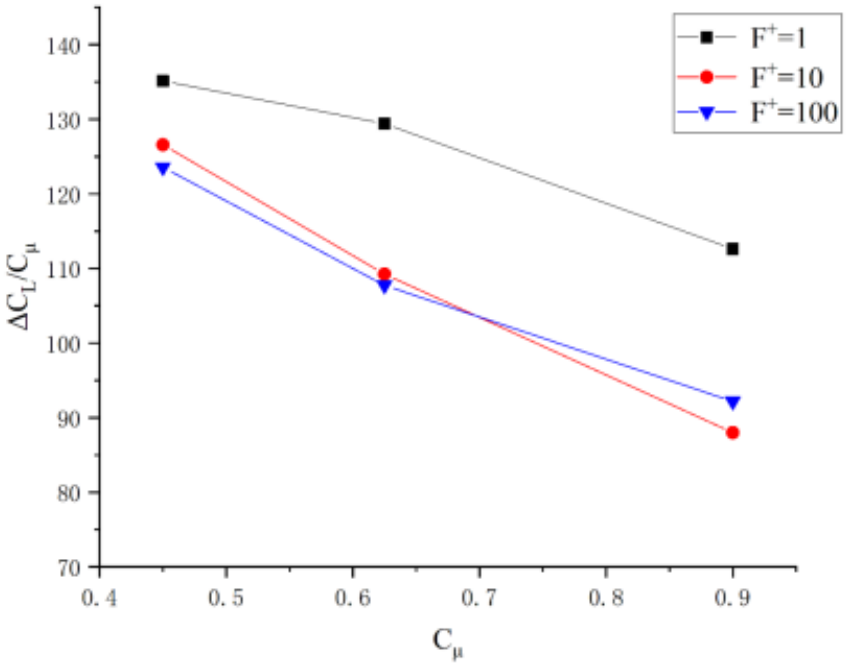

Figure 12. The effect of increasing momentum coefficient on control effectiveness.

control with momentum coefficients of 0.45%, 0.625%, and 0.9%. From these figures, we can see that under low momentum, the separation point moved to x/c = 0.7 due to poor control effect, but flow control has been basically achieved under the other two high momentum coefficients. The fluid velocity on the upper surface of the airfoil increases with the increase of momentum coefficient, which increases the negative pressure on the upper surface and the lift coefficient.

From the variation relationship of $\Delta C_L/\Delta C_\mu$ in **Figure 12**, we can see that as the momentum coefficient increases, the control efficiency for lift improvement decreases, and the control efficiency at oscillation frequency $F^+ = 1$ is higher than that under other control conditions.

3.2. The Influence of Oscillation Frequency on Control Effectiveness

Figure 13 shows the average velocity flow field at different oscillation frequencies

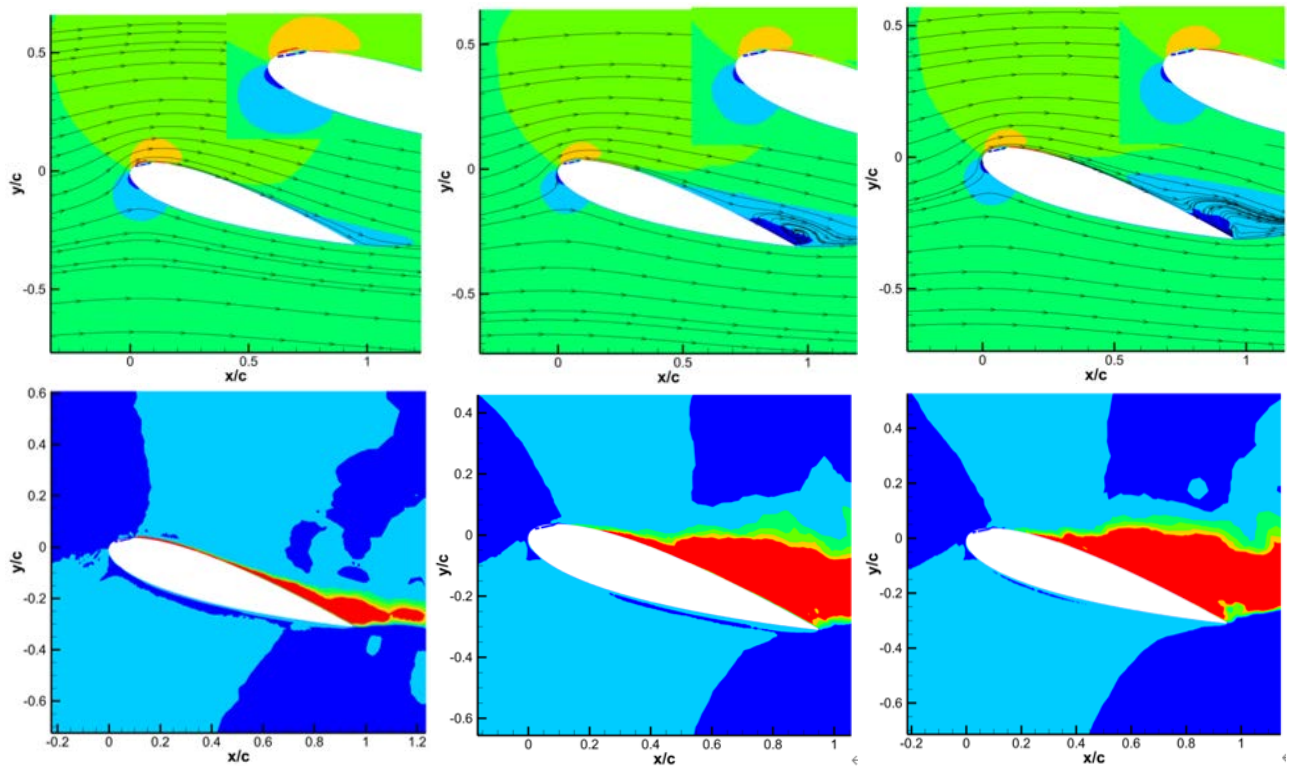

Figure 13. Average flow velocity and flow field at oscillation frequencies of 1 (left), 10 (center), and 100 (right).

of 18˚ attack angles with a momentum coefficient of 0.9%. It can be seen that the flow separation control effect is best when $F^+ = 1$, as the separation vortex disappears and the flow separation is completely suppressed. But when $F^+ = 10$ and 100, its control effect is not sufficient to completely control flow separation. And we can observe that compared to $F^+ = 10$, 100, when $F^+ = 1$, there is a significant increase in high-speed fluid at the position before the installation point of the sweeping jet actuator at the leading edge of the wing. The high-speed fluid at the leading edge can enhance the negative pressure on the upper wing surface, thereby increasing the lift coefficient. Meanwhile, the better the control effect of flow separation, the smaller the size of the separated vortex, and the better its lift enhancement effect. These may be the reasons why $F^+ = 1$ enhances lift the best.

In addition, a pair of alternating vortices is generated at the outlet of the sweeping jet actuator, and when they average over time, a pair of opposite rotating vortices will appear. **Figure 14** provides an example of the expected flow vortices and their directions in the current study. The function of these vortices is to bring high momentum flow from free flow into the boundary layer.

4. Conclusions

Through the application of the new sweeping jet actuator designed in this article to flow control on the NACA0018 airfoil, we investigated the effects of the oscillation frequency and jet momentum coefficient of the sweeping jet actuator on the flow control effect. The article concludes that:

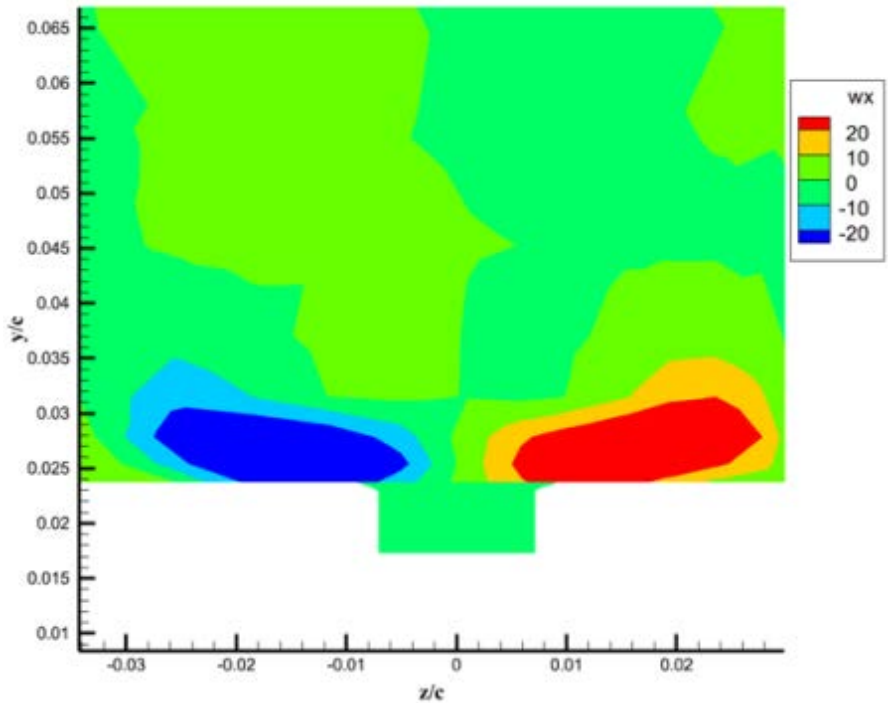

Figure 14. Alternating vortex at the outlet of a sweeping jet actuator.

1) At the same oscillation frequency, the flow control effect becomes better with the increase of momentum coefficient, but the efficiency of improving lift coefficient gradually decreases.

2) Under the same momentum coefficient, all three oscillation frequencies can delay flow separation, and when the oscillation frequency $F^+ = 1$, there is a significant improvement in lift coefficient.

As an active flow control technology with the advantage of no moving components, this study will help sweeping jet actuator play a better role in the field of flow control.

Conflicts of Interest

The authors declare no conflicts of interest regarding the publication of this paper.

References

[1] Zhu, Z.Q., Ju, S.J. and Wu, Z.C. (2016) Laminar Flow Active/Passive Control Technology. *Acta Aeronautica et Astronautica Sinica*, **37**, 2065-2090.

[2] Zhang, J., Liu, J.Y. and Zhang, B.Q. (2016) Experimental and CFD Study on the Mechanism of Supercritical Airfoil Drag Reduction with Micro Vortex Generators. *Journal of Experiments in Fluid Mechanics*, **30**, 37-41.

[3] Shi, Q. and Li, Y. (2010) Numerical Simulation on Action of Flow Control and Wave Drag Reduction Effect with Contour Bump Located on the Supercritical Airfoil. *Acta Aerodynamica Sinica*, **28**, 462-465.

[4] Zhang, Z.H., Li, D. and Yang, Y. (2017) Passive Flow Control of Multi-Element Airfoils Using Slat Mini-Trailing Edge Device. *Acta Aeronautica et Astronautica Si-*

nica, **38**, 129-139.

[5] Zhang, Z.Y., Wang, T.T., Chen, Z.H. and Jiang, F. (2020) The Effect of Blowing/Suction Jet on the Aerodynamic Performance of Airfoil NACAOO12 at Low Reynolds Number. *Acta Aerodynamica Sinica*, **38**, 58-65.

[6] Wu, Y. and Li, Y.H. (2015) Progress and Outlook of Plasma Flow Control. *Progress and Outlook of Plasma Flow Control*, **36**, 381-405.

[7] Luo, Z.B., Xia, Z.X. and Deng, X. (2017) Research Progress of Dual Synthetic Jets and Its Flow Control Technology. *Acta Aerodynamica Sinica*, **35**, 251-264.

[8] Florian, O., Rene, W., Christian, N. and Christian, O.P. (2019) Interaction between a Jet Emitted by a Fluidic Oscillator and a Crossflow at a Skew Angle. *AIAA Scitech 2019 Forum*, 7-11 January 2019.

[9] Daniel J.P., Eugene N.H., Matt G. (2021) Modal Analysis of a Sweeping Jet Emitted by a Fluidic Oscillator, *AIAA Aviation* 2021 *Forun*, 2-6 August 2021.

[10] Bartosz, J.S. and Kursat, K. (2017) Effects of Feedback Channels and Coanda Surfaces on the Performance of Sweeping Jet Actuator. 55*th AIAA Aerospace Sciences Meeting*, 9-13 January 2017.

[11] Jung, H.S. and Rajat, M. (2017) Computational Modeling and Analysis of Sweeping Jet Fluidic Oscillators, 47*th AIAA Fluid Dynamics Conference*, 5-9 June 2017.

[12] Arpit C., Kamal P. (2023) Control of Flow Separation using Fluidic Oscillators on a NACA 0015 Aerofoil, *AIAA Aviation 2023 Forum*, 12-16 June 2023.

[13] Sun, Q.X., Wang, W.B. and Huang, Y. (2022) Oscillation Characteristics of Suction and Oscillatory Blowing Actuator. *Acta Aeronautica et Astronautica Sinica*, **43**, 221-238.

[14] Zou, J.P., Liu, X.W., Cheng, J. and Li. J.L. (2017) Analysis and Improvement of Energy Efficiency of Jet Wall-Attached Oscillator. *Journal of Dalian University of Technology*, **57**, 233-240.

[15] Zhou, L.L., Wang, S.Q. and Wen, X. (2022) Working Characteristics of a Fluidic Oscillator with High Frequency and High Speed. *Journal of Aerospace Power*, **37**, 877-885.

[16] Alexander, S., Anthony, P.P. and Jeffrey, P.B. (2023) Leading-Edge Active Flow Control Enabled by Curved Fluidic Oscillators. *AIAA Journal*, **61**. https://doi.org/10.2514/1.J062329